JOURNAL OF SOLID STATE CHEMISTRY **98**, 151–158 (1992)

Crystal Structure and Thermolysis of $K_2(H_5O_2)Al_2F_9$

A. LE BAIL, H. DUROY, AND J. L. FOURQUET

Laboratoire des Fluorures, URA CNRS 449, Faculté des Sciences,
Université du Maine, 72017 Le Mans Cedex, France

Received July 9, 1991; in revised form November 15, 1991

$K_2(H_5O_2)Al_2F_9$ is formed by a spontaneous decomposition process from $K(H_3O)_2AlF_6$. The structure is determined from X-ray powder diffraction data and refined using the Rietveld method: space group *Pbam*; $Z = 4$; $a = 11.5418(7)$ Å, $b = 11.3437(7)$ Å, and $c = 3.6733(2)$ Å; $R_B = 0.035$, $R_P = 0.085$. The network is built up from $[Al_2F_9]_n^{3n-}$ double condensed chains of *trans*-corner-linked AlF_6 octahedra, running along the *c* axis. KF_6 trigonal prisms connect the chains, delimiting tunnels larger than those of the mineral hollandite, where $[H_5O_2]^+$ hydroxonium ions are located with some disorder. The thermolysis leads to an unidentified $KAlF_4$ form, stable in the 50–250°C range, then to β-$KAlF_4$ isotypic with β-$RbAlF_4$, tetragonal-tungsten-bronze-related, and finally to α-$KAlF_4$.

Introduction

The material formulated "K_2HAlF_6" synthesized by Kolditz *et al.* (*1*) was recently shown to be $K(H_3O)_2AlF_6$ from elemental analysis (*2*). This was confirmed by a structure determination (*3*) showing a relation with elpasolite (K_2NaAlF_6). The thermolysis of $K(H_3O)_2AlF_6$, investigated by X-ray diffraction and IR spectroscopy (*4*), seemed to reveal a hydrated phase $KAlF_4 \cdot 0.5H_2O$ and two anhydrous unknown $KAlF_4$ compounds (noted A_1 and A_2 in Ref. (*4*)), with the end product being the well known tetragonal $KAlF_4$ form (*5*), with disconnected perovskite layers, denoted α-$KAlF_4$ here. The structures of the new phases were not determined due to the lack of a single crystal; cell propositions from X-ray powder data were given (*4*).

In order to try to clarify this situation, we decided to make use of recent advances in the possibilities of structure determination from powder diffraction data. We have demonstrated elsewhere (*6*) that "$KAlF_4 \cdot 0.5H_2O$" described in (*2, 4*) is in fact $KAlF_4 \cdot 0.66H_2O$. Its structure is built up from disconnected hexagonal-tungsten-bronze-like-layers (HTB). On heating, $KAlF_4 \cdot 0.66H_2O$ progressively loses water, passing through an intermediate state with formulation $KAlF_4 \cdot 0.33H_2O$, also HTB-related, previously denoted A_1-$KAlF_4$ in (*4*). Near 200°C, the A_2 phase is formed with really the $KAlF_4$ formulation; its structure is determined here for the first time; it is denoted β-$KAlF_4$. Finally, the tetragonal well known α-$KAlF_4$ phase is detected.

This paper reports on the crystal structure of $K_2(H_5O_2)Al_2F_9$, determined and refined from X-ray powder diffraction data, and on its thermal decomposition. As with $KAlF_4 \cdot 0.66H_2O$, $K_2(H_5O_2)Al_2F_9$ is obtained from the $K(H_3O)_2AlF_6$ precursor.

Experimental

$K_2(H_5O_2)Al_2F_9$ in powder form is obtained at room temperature from a slow spontane-

0022-4596/92 $5.00

ous decomposition process of $K(H_3O)_2AlF_6$ single crystals following the global reaction scheme

$$2\,K(H_3O)_2AlF_6 \rightarrow K_2(H_5O_2)Al_2F_9 + 3HF + 2H_2O.$$

This new phase was not previously identified in the thermal decomposition study of $K(H_3O)_2AlF_6$ (*2, 4*), leading to an amorphous phase stable on a large temperature range (up to 140°C) before crystallization of $KAlF_4 \cdot 0.66H_2O$. The thermolysis of $K_2(H_5O_2)Al_2F_9$ was followed by DTA (Netsch 404S), TG (Perkin–Elmer TGS2, Ar flow), and temperature resolved X-ray powder diffractometry (TRXD) (Siemens D5000 θ/θ diffractometer equipped with an Elphyse position-sensitive detector and an Anton Parr temperature attachment).

The TG experiment realized at 5°C/min presented an unique weightloss stage in the 50–150°C range. The measured weight change (15.2%) was consistent with the calculated one (16.5%) according to the following global reaction:

$$K_2(H_5O_2)Al_2F_9 \rightarrow 2KAlF_4 + 2H_2O + HF.$$

The DTA experiment was realized with the same heating rate as the TG one. A large endothermic event (90–200°C) culminating at 160°C was detected, which can be associated with the decomposition process. This event was followed by an exothermic smaller one (240–270°C) with maximum at 256°C, suggesting a phase transition between two $KAlF_4$ polymorphs. Melting was observed at 550°C.

The TRXD experiment was performed following very different kinetic conditions than the TG and DTA ones. The sample was dusted on a platinum foil serving as heating source in a chamber pumped under vacuum, then filled with dried helium. A light He flow was maintained during the experiment. The time interval between successive powder patterns was 7200 sec including a measuring time of 6600 sec; the temperature was increased by steps of 10°C starting from 30°C up to 350°C. Co$K\alpha$ radiation was used, measurements were from 10 to 140°2θ by nearly 0.03°2θ steps. A linear contour scale plot is shown Fig. 1; patterns selected at some characteristic temperatures are gathered Fig. 2. The experiment will be commented in the following paragraph.

Interpretation of the TRXD of $K_2(H_5O_2)Al_2F_9$

The thermal decomposition of $K_2(H_5O_2)Al_2F_9$ gives rise to a new $KAlF_4$ form (which will be denoted $KAlF_4$-X). This new form is stable from 50°C up to 250°C in the TRXD kinetic conditions (see Fig. 1). Its formulation is established from the agreement between theoretical and observed mass loss during TG experiments and from its irreversible transformation into β- and α-$KAlF_4$. From the powder data, we did not recognize any isotypic material. $KAlF_4$-X presents medium X-ray line broadening implying nonnegligible crystallite size or/and strain effects. Moreover, the poor crystallinity remains unchanged after a long heating near 230°C. In spite of these unfavorable conditions, we have tried to define the cell by automatic indexing; however, as we have failed to determine the structure up to now, we present our results as being dubious. The most probable cell proposition obtained from the TREOR program (*7*) was orthorhombic with a = 11.902(4), b = 8.324(2), c = 7.247(1) Å (room temperature). The space group could not be established unequivocally.

During the TRXD, $KAlF_4$-X appears to decompose almost simultaneously into α- and β-$KAlF_4$ near 250°C (see Fig. 1). β-$KAlF_4$ is stable up to 340°C, then transforms into the α-form. Although β-$KAlF_4$ is always mixed with α-$KAlF_4$, the simplicity of the latter allowed to obtain a sufficient number of reflection positions for automatic indexing. The I-centered tetragonal cell pro-

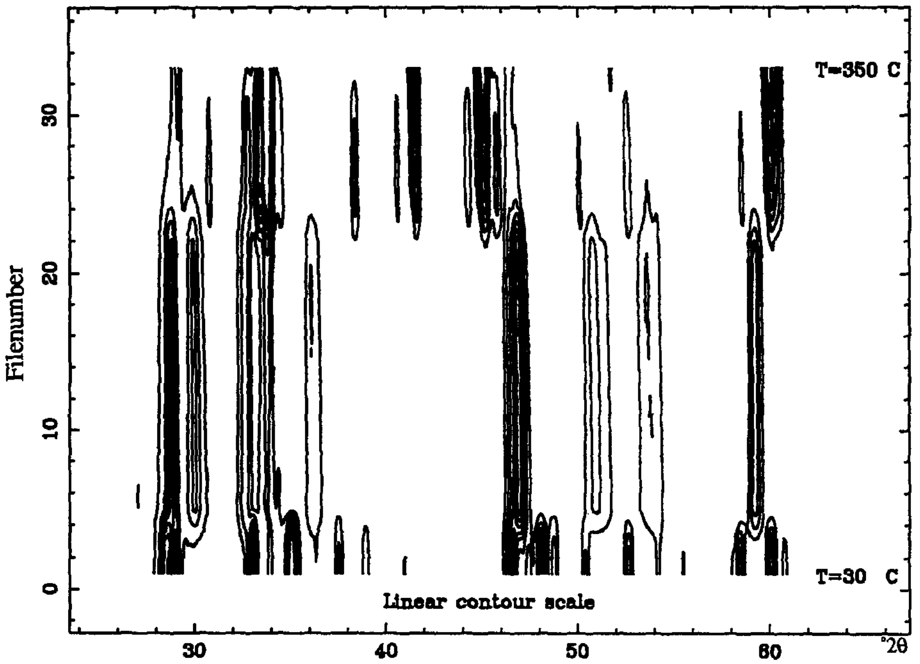

FIG. 1. Contour plot (intensity) of the X-ray powder diffraction patterns (Co*K*α) as a function of temperature (°C).

posed by the DICVOL program (*8*, *9*), with parameters $a = 11.568(1)$ and $c = 12.035(2)$ Å (at room temperature), suggested an isotypy with the tetragonal-tungsten-bronze-related β-$RbAlF_4$ (*10*) and β-$CsAlF_4$ (*11*) (S.G. $I\bar{4}c2$). This hypothesis was confirmed by a multipattern Rietveld refinement including the two $KAlF_4$ phases at 320°C. Unfortunately, the α-phase being largely dominant, the results quality is too low to give here the atomic coordinates of the β-phase. It was verified however that these coordinates did not deviate far from those of the β-$RbAlF_4$ starting model (refined cell parameters for β-$KAlF_4$ were $a = 11.6339(6)$, $c = 12.1948(9)$ Å at 320°C). Although the indexation is very different from that given for the A_2-phase in (*4*), we checked by comparison of the d_{hkl} values from Ref. (*12*) that the A_2-phase was β-$KAlF_4$. In the case of β-$RbAlF_4$, the $\beta \rightarrow \alpha$ irreversible, nondestructive, and topotactic phase transition at 315°C was explained by a concerted $\pi/4$ rotation, around the c-axis, of four octahedra groups (*10*); this explanation is probably convenient for the $\beta \rightarrow \alpha$-$KAlF_4$ transition too. One can note that α-$KAlF_4$ appearing in this experiment is not free from antiphase domains up to 350°C, as ascertained by the strong broadening of some *hkl* reflections such that $h + k = 2n + 1$, with $l \neq 0$ (*13*).

Structure Determination of $K_2(H_5O_2)Al_2F_9$

A powder diffraction pattern of $K_2(H_5O_2)Al_2F_9$ was recorded, at room temperature, on a PW1380 Philips diffractometer, automated with a DACO system. Indexing was realized by using the TREOR program (*7*) applied to the first 20 detected reflections. The most probable cell proposition was orthorhombic with figures of merit

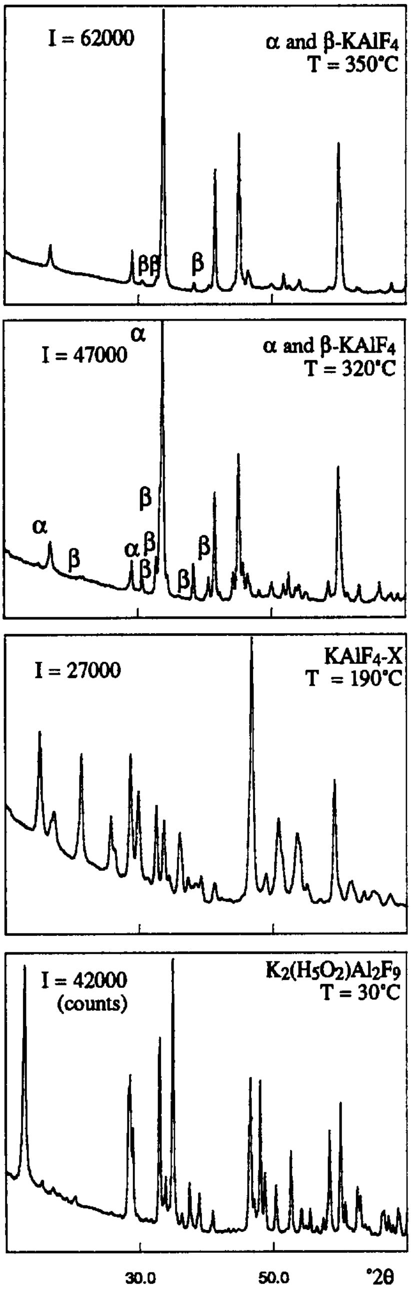

FIG. 2. Selected X-ray powder diffraction patterns (Co$K\alpha$) at some characteristic temperatures.

(*14, 15*) $M_{20} = 24$, $F_{20} = 36(0.012, 49)$. From the observed reflection conditions, the space groups *Pbam* or *Pba*2 could be selected. Individual reflection intensities were then extracted from the powder pattern by using a local cell-constrained profile fitting program (*16*).

Among the 302 reflections, 223 were selected because they had no neighbouring reflection at less than 0.04°2θ on the powder pattern. Straightforward application of the direct method facilities of the SHELXS-86 program (*17*) on this data set gave a proposition for the coordinates of the K, Al, and four independent F atoms, using the centric *Pbam* space group. Scattering factors and anomalous dispersion terms for K^+, Al^{3+}, and F^- were taken from the "International Tables for X-ray Crystallography" (*18*), and for O^{2-} from (*19*). Refinements using the SHELX-76 program (*20*) led to $R = 0.32$, the remaining F atom and the oxygen atom were located from a Fourier difference map. An $R = 0.20$ was obtained by refining the whole structure using this data set. The final refinements were from the Rietveld method (*21, 22*), using a program adapted to X-ray diffraction (*16*), taking into account the presence of a few percents of $KAlF_4 \cdot 0.66H_2O$ (all atomic coordinates were kept fixed, refining independently only a scale factor for this impurity estimated to represent no more than 1 or 2% of the sample volume). Using isotropic thermal motion, the conventional Rietveld discrepancy factors were $R_B = 0.049$ and $R_P = 0.098$. All atoms occupied 2*b*, 4*h*, or 4*g* positions (Wyckoff notation) of the *Pbam* space group, i.e., their *z* coordinates were fixed at either $\frac{1}{2}$ or 0. The *B* factors were considered as being abnormally high, particularly for the O atom ($B = 7.7(2)$ Å^2), so the *Pba*2 noncentrosymmetrical space group was tested. The origin along the *c*-axis was determined by keeping fixed the potassium atom at $z = 0$. Then the *z*-coordinates of all the other atoms became free parameters in the *Pba*2 space group. A significative improvement of the *R* factors was obtained since they dropped to $R_B = 0.039$ and $R_P = 0.088$

(with seven supplementary parameters). However, only the O atom presented a shift of the z-coordinate (from $\frac{1}{2}$ or 0) clearly greater than the estimated standard deviation, changing from $z = \frac{1}{2}$ to $z = 0.371(4)$, its B factor decreasing to 5.4(2) Å^2. We have considered afterwards the hypothesis of a possible static disorder of the (H_5O_2) group allowing to keep the centrosymmetrical space group. The O atoms were considered to possibly half-occupy the general 8i positions of the *Pbam* space group. Thus, with only one supplementary parameter, refinements led to even lower R values than using the *Pba*2 space group with seven supplementary parameters. Moreover, the B value for the oxygen atom became comparable to those of the F atoms. This was believed to be conclusive that the structure of $K_2(H_5O_2)Al_2F_9$ was better described using the *Pbam* centrosymmetrical space group than using the *Pba*2 space group. No evidence for a supercell with a multiple c-axis could be found on the powder pattern. Table I summarizes the conditions of structure determination and refinement. The agreement between the observed and calculated patterns can be checked on Fig. 3. The atomic coordinates are gathered Table II; selected interatomic distances and angles are given Table III.

TABLE I

CONDITIONS OF X-RAY POWDER DATA MEASUREMENT, STRUCTURE DETERMINATION AND RIETVELD REFINEMENT OF $K_2(H_5O_2)Al_2F_9$

Space group		*Pbam*
Z		4
Cell parameters (Å)	a	11.5418(7)
	b	11.3437(7)
	c	3.6733(2)
Volume (Å^3)		480.93(7)
2θ range (°)		5-100
Step scan (°2θ)		0.02
Time/step (s)		12.
Number of *hkl*		301[a]
Number of refined parameters		
total		34
xyz coordinates		14
Zeropoint (°2θ)		0.036(2)
Preferred orientation[b]		1.110(2)
direction		001
Profile parameters (see equation 1 in (*16*))	U_1	0.20[d]
	V_1	−0.10(1)
	W_1	0.154(5)
	U_2	0.00[d]
	V_2	−0.05(4)
	W_2	1.11(2)
	C	−0.021(2)
	D	−0.18(1)
	a	140
	l	69
Discrepancy factors[c]		
from pattern fitting	R_P	0.080
	R_{WP}	0.089
from Rietveld refinement	R_B	0.035
	R_P	0.085
	R_{WP}	0.095
	R_E	0.035

[a] 110 reflection at low angle excluded.

[b] March's model (*23*)

[c] R_P and R_{WP} values are calculated after background subtraction.

[d] Fixed value.

Structure Description of $K_2(H_5O_2)Al_2F_9$ and Discussion

A projection of the structure along the small c-axis is given Fig. 4. The network is built up from chains of *trans*-corner-linked AlF_6 octahedra associated in order to form double chains, obeying the $(Al_2F_9)_n^{3n-}$ formulation. These chains run along the c-axis. Each AlF_6 octahedron shares three corners with six KF_6 trigonal prism (TP). Each TP links two different $(Al_2F_9)_n^{3n-}$ double chains and shares its two triangular faces with two other adjacent TP, forming columns of TP in the c-direction. In this way, the network is tridimensional. The linkage scheme gives rise to large octogonal tunnels parallel to the c-axis, having irregular sections. These tunnels look like those of the mineral hollandite (*24*). However they are not identical, since the tunnels develop along an axis having the O–O length in hollandite. Nevertheless, in $K_2(H_5O_2)Al_2F_9$, the cavities inside

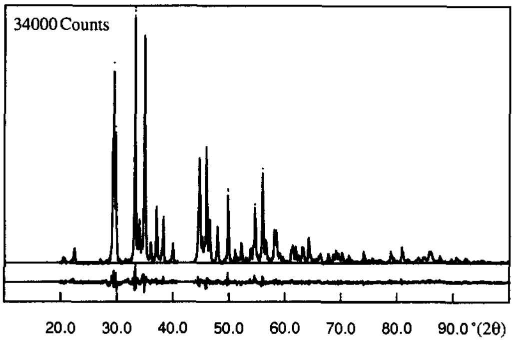

FIG. 3. Comparison of observed (···) and calculated (—) intensities at room temperature. The difference pattern appears below, at the same scale (Cu$K\alpha$).

TABLE III

SELECTED INTERATOMIC DISTANCES (Å) AND ANGLES (°) FOR $K_2(H_5O_2)Al_2F_9$

AlF_6 Octahedron ⟨Al–F⟩ = 1.800

Al	F(1)	F(2)	F(4)	F(3)	F(3)	F(5)
F(1)	**1.749(4)**	2.541(4)	2.534(4)	2.601(3)	2.601(3)	3.595(3)
F(2)	92.7(4)	**1.762(4)**	3.522(4)	2.548(3)	2.548(3)	2.491(3)
F(4)	92.3(4)	174.9(3)	**1.764(4)**	2.541(3)	2.541(3)	2.499(3)
F(3)	92.9(2)	90.1(2)	89.7(2)	**1.839(1)**	3.673(4)	2.539(2)
F(3)	92.9(2)	90.1(2)	89.7(2)	174.2(3)	**1.839(1)**	2.539(2)
F(5)	180.0(3)	87.3(3)	87.6(3)	87.1(1)	87.1(1)	**1.845(2)**

K Trigonal prism

2×	K–F(1)	2.619(3)
2×	K–F(2)	2.693(3)
2×	K–F(4)	2.719(3)

⟨K–F⟩ = 2.677

Oxygen bonding scheme

O–O	2.509(6)
or	2.318(7)
O–F(2)	2.517(6)
O–F(4)	2.542(5)
F(4)–O–F(2)	112.3(3)

the tunnels have almost a cubic shape as those in the hollandite with 8 of the 16 fluorine atoms of the irregular octogonal prisms being at shorter distance of the cavity center than the 8 others (3.69–3.78 Å to be compared to nearly 3 Å in the hollandite). The $(H_5O_2)^+$ hydroxonium ions are located near the octogonal faces; from the distances and angles there is no doubt on the hydrogen bonding scheme which involves the F(4) and F(2) fluorine atoms building the cubic cavity. However, the disorder already mentioned leads to two couples of solutions for the positions of the H_5O_2 group. Such a disorder is not surprising owing to the cavity size. In the hollandite case, there is a great deal of variation in the degree of filling the tunnels and in the exact position of the occupied sites, and even in the symmetry of the structure (tetragonal but some are monoclinic). In $K_2(H_5O_2)Al_2F_9$ the two couples of two possible configurations for the H_5O_2 group are the following: the two oxygen atoms could be at the same z-value (both at $z = 0.37$ or at $z = -0.37$) or they could be at inverse z-coordinates. The O–O distances corresponding to these two configurations are quite different (respectively 2.32 and 2.51 Å). None of these distances shows a sufficiently good agreement with classical O–O distances for (H_5O_2) to make a choice. Among the very few other oxonium compounds, one can find, for instance $(H_5O_2)_3PW_{12}O_{40}$ (d_{O-O} = 2.370 Å) (*25*); $H_2SO_4 \cdot 6.5H_2O$ and $H_2SO_4 \cdot 8H_2O$ (2.448 and 2.447 Å) (*26*); $(H_5O_2)_2AlF_5 \cdot H_2O$ and $(H_5O_2)_3AlF_6$ (2.455 and 2.442 Å) (*27*); and in $(H_5O_2)BF_4$ (2.412 Å) (*28*). The O . . . F distances (see Table III) themselves are clearly shorter than those found in $(H_5O_2)_3AlF_6$ (2.590 and 2.604 Å) and in $(H_5O_2)_2AlF_5 \cdot H_2O$ (2.56 to 2.72 Å) or in $(H_5O_2)BF_4$ (2.615 to 2.874 Å). It

TABLE II

ATOMIC COORDINATES AND ISOTROPIC THERMAL PARAMETERS FOR $K_2(H_5O_2)Al_2F_9$

Atom	Site	x	y	z	B(Å^2)
K	4g	0.3564(2)	0.3156(2)	0	3.50(5)
Al	4h	0.1247(2)	0.1018(2)	$\frac{1}{2}$	2.15(5)
F(1)	4h	0.2430(3)	0.1982(4)	$\frac{1}{2}$	3.7(1)
F(2)	4h	0.0237(3)	0.2183(3)	$\frac{1}{2}$	3.4(1)
F(3)	4g	0.1188(3)	0.0963(3)	0	3.3(1)
F(4)	4h	0.2152(3)	0.9766(3)	$\frac{1}{2}$	3.3(1)
F(5)	2b	0	0	$\frac{1}{2}$	3.6(2)
O[a]	8i	0.0733(3)	0.4302(4)	0.369(2)	3.8(2)

[a] Site half occupied.

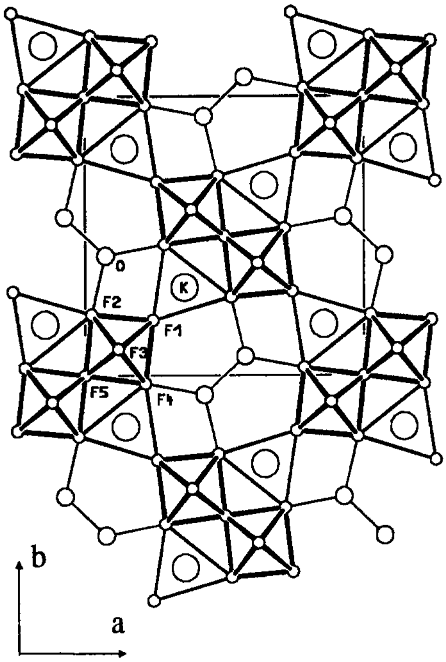

FIG. 4. (001) projection of the structure of $K_2(H_5O_2)Al_2F_9$. K atoms are the largest circles ($z = 0$); F atoms are the smallest, all F atoms but F(3) are at $z = \frac{1}{2}$; O atoms are the medium-size circles ($z = \pm 0.37$). The suggested hydrogen bonding scheme is represented by thin straight lines; AlF_6 octahedra represented by heavy lines and KF_6 trigonal prisms by medium-size lines.

is also to be noted that the O . . . F distances are out of the range 2.56–2.86 Å quoted by Simonov and Bukvetski (*29*) for O–H . . . F hydrogen bonding in metal-fluoride-hydrates involving H_2O molecules. Thus it is difficult to discuss more about the hydroxonium ion in this structure established from powder data. The hydrogen atoms were not located.

In spite of the problem of disorder and of the medium accuracy which can be expected from this study, it seems that the Al–F and K–F distances may be considered with some confidence. As frequently observed the bridging bonds (Al–F(3) and Al–F(5)) are longer than the terminal ones (Table III); the mean Al–F and K–F distances are very close to the sum of the ionic radii (*30*), the extreme distances deviate few from the means.

The topology of the double $(Al_2F_9)_n^{3n-}$ chains in $K_2(H_5O_2)Al_2F_9$ is simple, however, it is, to our knowledge, the first example of this kind in fluorides crystal chemistry. In the well known series including $KPbCr_2F_9$ (*31*) and $NaBaFe_2F_9$ (*32*), double infinite chains of similar formulation (but eventually different charge) are always *cis*-linked. The very original structure of $K_2(H_5O_2)Al_2F_9$ suggests the possibility of ionic exchange inside the tunnels. Further work is in progress in this direction.

Acknowledgement

The authors are very indebted to Dr. R. Retoux who performed many TXRD experiments.

References

1. L. KOLDITZ, U. BENTRUP, AND I. TITT, *Z. Chem.* **23**, 231 (1983).
2. U. BENTRUP AND L. KOLDITZ, *J. Thermal Anal.* **34**, 1413 (1989).
3. G. FRENZEN AND W. MASSA, *Acta Crystallogr., Sect. C: Cryst. Struct. Commun.* **C46**, 190 (1990).
4. U. BENTRUP AND L. KOLDITZ, *Z. Anorg. Allg. Chem.* **540/541**, 8 (1986).
5. J. NOUET, J. PANNETIER, AND J. L. FOURQUET, *Acta Crystallogr. Sect. B: Struct. Crystallogr. Cryst. Chem.* **B37**, 32 (1981).
6. J. L. FOURQUET, A. LE BAIL, H. DUROY, AND U. BENTRUP, to be published.
7. P. E. WERNER, L. ERIKSSON, AND M. J. WESTDAHL, *J. Appl. Crystallogr.* **18**, 367 (1985).
8. D. LOUER AND M. LOUER, *J. Appl. Crystallogr.* **5**, 271 (1972).
9. D. LOUER AND R. VARGAS, *J. Appl. Crystallogr.* **15**, 542 (1982).
10. J. L. FOURQUET, F. PLET, AND R. DE PAPE, *Acta Crystallogr. Sect. B: Struct. Crystallogr. Cryst. Chem.* **B36**, 1997 (1980).
11. U. BENTRUP, A. LE BAIL, H. DUROY, AND J. L. FOURQUET, submitted.
12. U. BENTRUP, private communication.
13. A. GIBAUD, A. LE BAIL, AND A. BULOU, *J. Phys. C: Solid State Phys.* **19**, 4623 (1986).
14. P. M. DE WOLF, *J. Appl. Crystallogr.* **1**, 108 (1968).
15. G. S. SMITH AND R. L. SNYDER, *J. Appl. Crystallogr.* **12**, 60 (1979).

16. A. Le Bail, H. Duroy, and J. L. Fourquet, *Mater. Res. Bull.* **23,** 447 (1988).
17. G. M. Sheldrick, *in* "Crystallographic Computing 3: Data Collection, Structure Determination, Proteins and Databases" (G. M. Sheldrick, C. Kruger, and R. Goddard, Eds.), p. 184, Oxford, Clarendon Press (1985); G. M. Sheldrick, *Acta Crystallogr., Sect. A: Found. Crystallogr.* **A46,** 467 (1990).
18. *"International Tables for X-ray Crystallography,"* Vol. IV, Kynoch Press, Birmingham (1974).
19. T. Suzuki, *Acta Crystallogr.* **13,** 279 (1960).
20. G. M. Sheldrick, "SHELX-76, A Program for Crystal Structure Determination," Univ. of Cambridge (1976).
21. H. M. Rietveld, *Acta Crystallogr.* **22,** 151 (1967).
22. H. M. Rietveld, *J. Appl. Crystallogr.* **2,** 65 (1969).
23. A. March, *Z. Kristallogr.* **81,** 285 (1932).
24. A. Bystrom and A.-M. Bystrom, *Acta Crystallogr.* **3,** 146 (1950).
25. G. M. Brown, M. R. Noe-Spirlet, W. R. Busing and H. A. Levy, *Acta Crystallogr., Sect. B: Struct. Crystallogr. Cryst. Chem.* **B33,** 1038 (1977).
26. D. Mootz and A. Merschenz-Quack, *Z. Naturforsch.* **B,** 1231 (1987).
27. D. Mootz, E. T. Oellers, and M. Wiebcke, *Acta Crystallogr., Sect. C: Cryst. Struct. Commun.* **C44,** 1334 (1988).
28. D. Mootz and M. Steffen, *Z. Anorg. Allg. Chem.* **482,** 193 (1981).
29. V. I. Simonov and Bukvetski, *Acta Crystallogr., Sect. B: Struct. Crystallogr. Cryst. Chem.* **B34,** 355 (1978).
30. R. D. Shannon, *Acta Crystallogr., Sect. A: Cryst. Phys. Diffr. Theor. Gen. Crystallogr.* **A32,** 751 (1976).
31. M. Vlasse, J. P. Chaminade, J. M. Dance, M. Saux, and P. Hagenmuller, *J. Solid State Chem.* **41,** 272 (1982).
32. G. Ferey, M. Leblanc, A. De Kozak, M. Samouel, and J. Pannetier, *J. Solid State Chem.* **56,** 288 (1985).